

# Interaction of a Fluorescent Acyldicholine with the Nicotinic Acetylcholine Receptor and Acetylcholinesterase

MICHAEL B. BOLGER,<sup>1</sup> VINCENT DIONNE, JOHN CHRIVIA,<sup>2</sup> DAVID A. JOHNSON,<sup>3</sup> AND PALMER TAYLOR

*Division of Pharmacology, M-013 H, University of California, San Diego, La Jolla, California 92093*

Received August 26, 1983; Accepted March 12, 1984

## SUMMARY

A fluorescent acyldicholine, bis-(choline)*N*-[4-nitrobenzo-2-oxa-1,3-diazol-7-yl]-imino-dipropionate (BCNI), was synthesized and its capacity to associate with acetylcholinesterase and the nicotinic acetylcholine receptor examined. The fluorescent bisquaternary diester competitively inhibits acetylcholinesterase with a  $K_i$  of 0.46  $\mu\text{M}$ . Binding is accompanied by a large decrease in BCNI fluorescence and a 40% reduction in enzyme tryptophanyl fluorescence due to spectral overlap between BCNI absorption and the fluorescence emission of tryptophanyl residues on the enzyme. BCNI titrations show a stoichiometry of one site per subunit and a dissociation constant of 0.2  $\mu\text{M}$ . BCNI also inhibits the initial rate of  $\alpha$ -toxin binding to the membrane-associated nicotinic acetylcholine receptor and yields a protection constant ( $K_p$ ) of 0.26  $\mu\text{M}$ . Prior exposure of BCNI to the receptor increases the affinity of the complex, and after equilibration  $K_p$  is found to be 0.11  $\mu\text{M}$ . Fluorescence titrations reveal that BCNI binds with 1:1 stoichiometry to  $\alpha$ -toxin sites on the receptor with a dissociation constant of 0.22  $\mu\text{M}$ . Agonists and antagonists, but not local anesthetics, compete with BCNI binding. BCNI behaves as a competitive antagonist on receptors from the snake neuromuscular junction and from BC3H-1 cells. The 4-nitrobenzo-2-oxa-1,3-diazole fluorophore in BCNI shows a hypsochromatic shift and an enhancement of quantum yield when bound to the receptor but is quenched when associated with acetylcholinesterase. Thus, despite the similarity in dissociation constants, the fluorophore exists in very different environments when bound to the two proteins.

## INTRODUCTION

Since the initial synthesis of dansylethyltrimethylammonium (1), a large number of fluorescent quaternary nitrogen compounds have been examined for their activity or inhibitory properties in cholinergic systems. Owing to the existence of more than a single type of binding site on both acetylcholinesterase (2, 3) and the nicotinic AChR<sup>4</sup> (4-6) and the observations that multiple states of both proteins can be distinguished by fluorescent ligands (7-9), the design of the ligand and its specificity are critical to the information that is likely to emerge

This work was supported in part by United States Public Health Service Grants GM 18360 and GM 24437.

<sup>1</sup> Recipient of Fellowship Award GM 06410 and Basic Science Research Grant Award S07-RR-05792. Present address, School of Pharmacy, PSC 700, University of Southern California, Los Angeles, Calif. 90033.

<sup>2</sup> Present address, Department of Pharmacology, University of Washington, Seattle, Wash. 98145.

<sup>3</sup> Present address, Division of Biomedical Sciences, University of California, Riverside, Calif. 92521.

<sup>4</sup> The abbreviations used are: AChR, acetylcholine receptor; NBD-Cl, 4-chloro-7-nitrobenzo-2-oxa-1,3-diazole; TLC, thin layer chromatography; BCNI, bis-(choline)*N*-[4-nitrobenzo-2-oxa-1,3-diazol-7-yl]-iminodipropionate; PMR, proton magnetic resonance.

from a spectroscopic study. Most of the fluorescent compounds which act at the agonist-antagonist site on the receptor have been acylcholine derivatives containing the chromophore in an extended, hydrophobic acyl chain (10-15). Although many of these compounds retain agonist activity, they also block receptor function noncompetitively (15). This latter action, which is characteristic of many local anesthetics, appears to be a consequence of binding to sites distinct from the agonist-antagonist site on the receptor.

An alternative approach to the development of a fluorescent agonist or antagonist for the nicotinic AChR would entail modification of the basic bisquaternary structure of decamethonium. Decamethonium, itself, is a partial agonist (16), and, even though *N*-substitution with larger alkyl groups confers to the molecule an enhanced affinity as an antagonist, the efficacy of such congeners as agonists is lost (17, 18). On the other hand, suberyldicholine possesses an interquaternary distance similar to that of decamethonium and is a potent agonist (19). The structural basis for suberyldicholine's efficacy as an agonist probably arises from the dipolar carbonyl groups between the quaternary ammonium moieties and closer resemblance to acetylcholine. Hence, other ago-

nists or antagonists might be developed from the basic structure of a choline ester of a dicarboxylic acid.

By placing a relatively small fluorophore positioned between the two quaternary moieties, noncompetitive inhibition characteristic of the local anesthetics with large hydrophobic acyl chains should be minimized. Moreover, the fluorophore between the quaternary groups will assume an unambiguous position with respect to the macromolecular binding site. In this presentation, we describe the synthesis, spectroscopic properties, and pharmacological behavior of a congener of pimelyldicholine in which a 4-nitrobenzo-2-oxa-1,3-diazole moiety has been incorporated between the two quaternary groups.

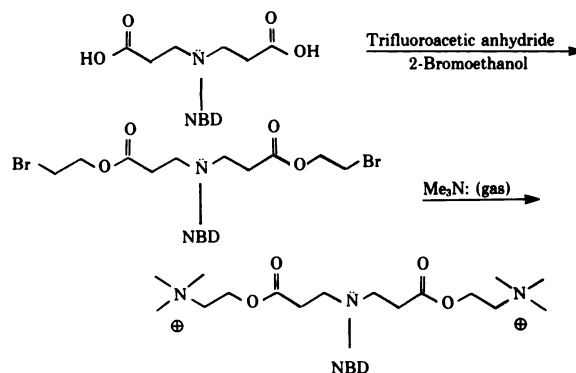
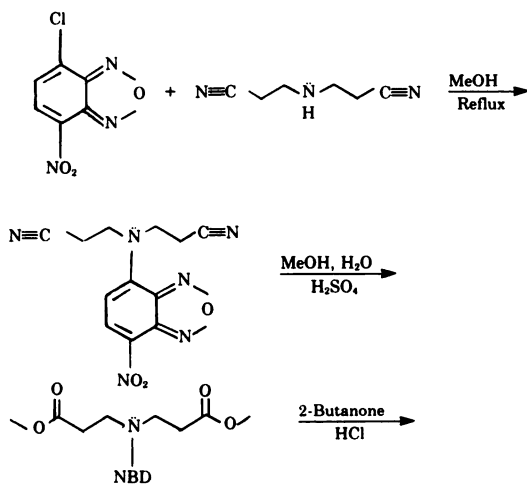
## EXPERIMENTAL PROCEDURES

**Materials.** Starting materials were purchased from the following suppliers: 3,3'-iminodipropionitrile, Pfaltz and Bauer (Stamford, Conn.); NBD-Cl, Aldrich Chemical Company (Milwaukee, Wisc.); trifluoroacetic acid anhydride, Sigma Chemical Company (St. Louis, Mo.); 2-bromoethanol, K&K Laboratories (Plainview, N. Y.); and trimethylamine gas, Matheson (East Rutherford, N. J.). Silica gel and cellulose adsorbents on plastic plates without fluorescent indicator (Eastman, Rochester, N. Y.) were utilized for TLC and electrophoresis, respectively. Carbamylcholine chloride and decamethonium bromide were products of Sigma Chemical Company. Lidocaine was obtained from K&K Laboratories. Suberyldicholine was a gift of Dr. G. Unger (Edinburgh, United Kingdom). [ $^{125}$ I]Monoiodo cobra  $\alpha$ -toxin (*Naja naja siamensis* 3) was prepared as described previously (6).

**Methods.** Electrophoresis of the charged intermediates and BCNI was conducted on cellulose in 10 mM sodium phosphate buffer (pH 7.0) containing 0.1 M NaCl (200 V, typically 7 mamp, run for 30 min). Migrations in the electric field are reported as  $R_F$  values relative to the farthest moving band. The intensities of the fluorescent bands were determined with an Aminco-Bowman spectrofluorometer equipped with a thin film scanner and interfaced to an IBM-PC microcomputer via a Tecmar analogue-to-digital computer. Melting points, determined with a Laboratory Devices MeltTemp capillary tube apparatus, are uncorrected.

PMR spectra were determined at 90 MHz with a Varian EM-390 spectrometer or at 500 MHz with the Bruker WM 500 at the Southern California Regional NMR facility, located at the California Institute of Technology. PMR chemical shift values are expressed in  $\delta$  units (parts per million) relative to tetramethylsilane internal standard. IR spectra were recorded with a Unicam SP 1000 spectrometer. Microanalyses were performed by the Microanalytical Laboratory, University of California (Berkeley, Calif.) and by Galbraith Laboratories, Inc. (Knoxville, Tenn.).

**Syntheses.** Syntheses of the compounds were carried out according to the following scheme:



4-(2',2''-Dicyano-N,N-diethylamino)-7-nitrobenzo-2-oxa-1,3-diazole.

Freshly redistilled 3,3'-iminodipropionitrile (58 g, 0.47 mole) was added to a stirred solution of 4-chloro-7-nitrobenzo-2-oxa-1,3-diazole (5 g, 25 mmoles) in 200 ml of anhydrous methanol. After 2 hr at room temperature, the dark red solution was heated to reflux for an additional 2 hr and then allowed to cool slowly to 0°.

The resulting golden solid (4.6 g) showed two fluorescent spots analyzed by TLC ( $\text{CHCl}_3/\text{acetone}$ , 75/25)  $R_{F_{\text{min}}}$  0.34,  $R_{F_{\text{max}}}$  0.43. This mixture was further purified in 300-mg batches by preparative high-pressure liquid chromatography (compressed to 35 atmos) [Waters Associates (Milford, Mass.), Prep LC System 500, single Prep PAK silica cartridge]. The solvent mixture for optimal separation of the two components ( $\text{CHCl}_3/\text{acetone}$ , 85/15) was determined by increasing the chloroform to produce  $R_F$  factors by TLC of 0.22–0.32 or less. For each injection, the column was loaded with 300 mg of crude material dissolved in 100 ml of solvent mixture and eluted at 100 ml/min. The two components were easily separated and collected in peaks of ~500 ml. Solvent was removed *in vacuo* from batches of the minor component (eluted first) to give 460 mg total, TLC ( $\text{CHCl}_3/\text{acetone}$ , 72/25)  $R_{F_{\text{min}}}$  0.42, PMR (60 MHz) ( $\text{acetone-d}_6$ )  $\delta$  3.1 (t,  $J = 7$  Hz, 2H,  $\text{CH}_2\text{—C}\equiv\text{N}$ ), 4.0 (t,  $J = 7$  Hz, 2H,  $\text{CH}_2\text{—N}$ ), 6.6 (d,  $J = 9$  Hz, 1H, 6—H—NBD), 8.5 (d,  $J = 9$  Hz, 1H, 5—N—NBD). This minor component appears to be the mononitrile. Solvent was removed *in vacuo* from the major component to give 2.9 g total (41%); m.p. 184–186°, TLC ( $\text{CHCl}_3/\text{acetone}$ , 75/25)  $R_{F_{\text{min}}}$  0.34. IR (mull, mineral oil), 2270  $\text{cm}^{-1}$  (nitrile), 1613  $\text{cm}^{-1}$  (olefin), 1555  $\text{cm}^{-1}$  (nitro). PMR (90 MHz) ( $\text{acetone-d}_6$ )  $\delta$  3.1 (t,  $J = 7$  Hz, 4H,  $\text{CH}_2\text{—C}\equiv\text{N}$ ), 4.5 [t,  $J = 7$  Hz, 4H, ( $\text{CH}_2$ ) $_2\text{—N}$ ], 6.8 (d,  $J = 9$  Hz, 1H, 6—H—NBD), 8.5 (d,  $J = 9$  Hz, 1H, 5—H—NBD).



Calculated: C 50.35, H 3.52, N 29.36

Found: C 50.56, H 3.70, N 29.20

4-(bis-(Methyl)-N,N-dipropionylamino)-7-nitrobenzo-2-oxa-1,3-diazole. Concentrated  $\text{H}_2\text{SO}_4$  (15 ml) was added slowly to an ice-cold suspension of the NBD-iminodipropionitrile (1 g, 3.5 mmoles) in 30 ml of methanol and 10 ml of water. The reaction mixture was brought to reflux (90°) and dissolved after 1 hr. After refluxing for 4 hr, the reaction mixture was stirred at room temperature for another 4 hr. The orange solid which formed in the flask was filtered, washed with cold water and hexane, dried, and recrystallized from acetone to give 851 mg (69%); m.p. 159–161°, TLC ( $\text{CHCl}_3/\text{acetone}$ , 75/25)  $R_{F_{\text{min}}}$  0.59. IR (mull, mineral oil), 1730  $\text{cm}^{-1}$  (ester), 1618  $\text{cm}^{-1}$  (olefin), 1555  $\text{cm}^{-1}$  (nitro). PMR (90 MHz) ( $\text{acetone-d}_6$ )  $\delta$  2.9 [t,  $J = 7$  Hz, 4H, ( $\text{CH}_2\text{—CO}_2\text{Me}$ ) $_2$ ], 3.7 [s, 6H, ( $\text{CH}_3\text{—O}$ ) $_2$ ], 4.35 [t,  $J = 7$  Hz, 4H, ( $\text{CH}_2$ ) $_2\text{—N}$ ], 6.5 (d,  $J = 9$  Hz, 1H, 6—H—NBD), 8.5 (d,  $J = 9$  Hz, 1H, 5—N—NBD).

4-(2',2''-Dicarboxy-N,N-diethylamino)-7-nitrobenzo-2-oxa-1,3-diazole. Concentrated HCl (8 ml) was added to a solution of the bis-(methyl)-NBD-iminodipropionate (1 g, 2.8 mmoles) dissolved in 100 ml of hot 2-butanone. The reaction mixture, in a 250-ml round-bottom flask fitted with a reflux condenser and fraction cutter, was allowed to reflux. After 5 hr of reflux and removal of 30 ml of distillate containing methanol at 2 and 4 hr, the reaction was stirred at room temperature for an additional 4 hr and the resulting orange precipitate was filtered and dried. Concentration of the reaction mixture produced a second

precipitate for a total yield of 797 mg (87%); m.p. 250–252° (decomp), electrophoresis (migration toward positive pole)  $R_{F_{90\%}}$  1,  $R_{F_{2\%}}$  0.51. IR (mull, mineral oil), 1715  $\text{cm}^{-1}$  (carbonyl stretch of H-bond dimer), 1615  $\text{cm}^{-1}$  (olefin), 1560  $\text{cm}^{-1}$  (nitro). PMR (60 MHz) (dimethyl sulfoxide- $d_6$ )  $\delta$  2.9 [broad t, 4H,  $(\text{CH}_2-\text{CO}_2)_2$ ], 4.3 [broad t, 4H,  $(\text{CH}_2)_2-\text{N}$ ], 6.65 (d, J = 9 Hz, 1H, 6—H—NBD), 8.5 (d, J = 9 Hz, 1H, 5—H—NBD).



Calculated: C 44.45, H 3.73, N 17.28

Found: C 44.56, H 3.82, N 17.13

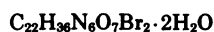
4-(bis-( $\beta$ -Bromoethyl)-N,N-dipropionylamino)-7-nitrobenzo-2-oxa-1,3-diazole. Cold trifluoroacetic acid anhydride (4.8 g, 23 mmoles) was added to the NBD-iminodipropionic acid (1.5 g, 4.6 mmoles) suspended at 0° in 25 ml of tetrahydrofuran which had been freshly distilled from  $\text{P}_2\text{O}_5$ . The reaction temperature was raised to 30°, and within 5 min the suspension had dissolved. 2-Bromoethanol (4.3 g, 35 mmoles) was added after 1.5 hr and the reaction mixture was stirred at room temperature overnight. Solvent was removed under reduced pressure to produce an oil which, when triturated with hexanes and a small amount of anhydrous methanol, yielded a dry orange solid. This solid contained substantial unreacted diacid as shown by TLC ( $\text{CHCl}_3/\text{acetone}$ , 75/25)  $R_{F_{30\%}}$  origin,  $R_{F_{70\%}}$  0.58. The desired compound was purified by preparative high-pressure liquid chromatography in a manner similar to that described for the NBD-iminodipropionitrile. The bromoethyl ester (1 g) was dissolved in 5 ml of column solvent ( $\text{CHCl}_3/\text{acetone}$ , 95/5) and injected onto the column in two 2.5-ml fractions. The elution was run at 100 ml/min, and the first peak emerging from the column was collected in 500 ml. The diacid contaminant was eluted with 100% acetone. The desired compound was obtained by solvent removal *in vacuo* from the two fractions followed by trituration of the residual oil with hexane and diethyl ether to give a reddish orange solid (545 mg, 22%); m.p. 69–71°, TLC ( $\text{CHCl}_3/\text{acetone}$ , 75/25)  $R_{F_{100\%}}$  0.59. IR (mull, mineral oil), 1730  $\text{cm}^{-1}$  (ester), 1618  $\text{cm}^{-1}$  (olefin), 1565  $\text{cm}^{-1}$  (nitro). PMR (60 MHz) (acetone- $d_6$ )  $\delta$  3.0 [t, J = 7 Hz, 4H,  $(\text{CH}_2-\text{CO}_2)_2$ ], 3.6 [t, J = 5 Hz, 4H,  $(\text{CH}_2-\text{Br})_2$ ], 4.4 [t, J = 7 Hz, 4H,  $(\text{CH}_2)_2-\text{N}$ ], 4.41 [t, J = 5 Hz, 4H,  $(\text{CH}_2-\text{OCOR})_2$ ], 6.55 (d, J = 9 Hz, 1H, 6—H—NBD), 8.4 (d, J = 9 Hz, 1H, 5—H—NBD).



Calculated: C 35.71, H 3.37, N 10.41, Br 29.70

Found: C 35.92, H 3.48, N 10.24, Br 29.51

4-(bis-(Choline)-N,N-dipropionylamino)-7-nitrobenzo-2-oxa-1,3-diazole dibromide. Acetonitrile (20 ml) dried over  $\text{P}_2\text{O}_5$  was distilled into a reaction vessel containing the bis-(bromoethyl)ester of NBD-iminodipropionate (250 mg, 0.47 mmole) while maintaining a dry nitrogen atmosphere. After distillation, the reaction vessel was fitted with a drying tube at the exhaust arm and a gas line for addition of dry trimethylamine while stirring at room temperature. After 7 hr, the accumulated reddish orange precipitate was filtered in a dry bag under nitrogen and washed with dry acetonitrile to give a hygroscopic orange solid (260 mg, 80%); m.p. 138–141°, electrophoresis (migration toward the negative pole)  $R_{F_{90\%}}$  1,  $R_{F_{2\%}}$  0.26. IR (mull, mineral oil), 1730  $\text{cm}^{-1}$  (carbonyl stretch of choline ester), 1615  $\text{cm}^{-1}$  (olefin), 1555  $\text{cm}^{-1}$  (nitro). PMR (500 MHz ( $^2\text{H}_2\text{O}$ ))  $\delta$  2.90 [t, J = 7.5 Hz, 4H,  $(\text{CH}_2-\text{CO}_2)_2$ ], 3.13 [s, 18H,  $((\text{CH}_3)_3-\text{N})_2$ ], 3.67 [t, J = 5 Hz, 4H,  $(\text{CH}_2)_2-\text{N}-(\text{Me}_3)$ ], 4.19 unresolved [t, 4H,  $((\text{CH}_2)_2-\text{N})$ ], 4.51 unresolved [t, 4H,  $((\text{CH}_2\text{OCOR})_2)$ ], 6.28 (d, J = 10 Hz, 1H, 6—H—NBD), 8.26 (d, J = 10 Hz, 1H, 5—H—NBD).



Calculated: C 38.16, H 5.82, N 12.14, Br 23.08

Found: C 37.88, H 5.96, N 11.94, Br 23.16

**Acetylcholinesterase activity and inhibition.** The 11 S form of acetylcholinesterase was purified to apparent homogeneity from the *Torpedo* electric organ by previously described affinity chromatographic procedures (20). The inhibitory potency of BCNI was monitored by inhibition of the rate of enzyme carbamylation by the fluorescent substrate, N-methyl-(7-dimethylcarboxy)quinolinium (21). All measurements

were conducted in 10 mM Tris-HCl buffer (pH 8.0) containing 0.1 M NaCl and 40 mM  $\text{MgCl}_2$ .

**Assay of ligand association with the cholinergic receptor.** Membranes enriched in cholinergic receptor were purified by a slight modification (22) of the procedures of Weiland *et al.* (6). Specific activities ranged between 1.5 and 3.1  $\mu\text{moles}$  of  $\alpha$ -toxin sites per gram of protein. Association of ligands with the receptor was monitored by their capacity to inhibit the initial rate of [ $^{125}\text{I}$ ]monoiodo  $\alpha$ -toxin binding (6). Initial rates were calculated from the slope of a bimolecular plot generated from several points over a 40-sec interval. [ $^{125}\text{I}$ ]Monoiodo  $\alpha$ -toxin addition either immediately followed addition of BCNI to the receptor or BCNI was allowed to equilibrate with the receptor for 20 min prior to  $\alpha$ -toxin addition. A comparison between measurements of immediate exposure to BCNI and after prior equilibration with BCNI allows one to assess the capacity of the ligand to convert the receptor to its high-affinity state (cf. ref. 6).

**Fluorescence titrations of BCNI association with the receptor.** Fluorescence measurements were conducted on a Farrand MK-1 spectrofluorometer equipped with excitation correction and linked to a Tektronix 4052 computer via a Trans Era analogue-to-digital converter. Spectra are corrected for photomultiplier sensitivity (22, 23). Titrations were carried out in 1-cm cuvettes using a temperature-jacketed, four-sample turreted compartment. This enabled the nearly simultaneous measurement of blank signals and the correction for light scatter, dilution, and inner filter effects (cf. refs. 20, 22, and 23). Except where noted, excitation and emission wavelengths were 290 and 519 nm, respectively. Fluorescence contributions of the free ligand were subtracted from the total fluorescence, and maximal fluorescence enhancement was calculated from extrapolation of reciprocal plots of fluorescence versus added ligand. Data of fluorescence enhancement versus ligand concentration were plotted directly or according to the Hill formulation, and the dissociation constants ( $K_D$ ) and Hill coefficients ( $n_H$ ) directly calculated. Stoichiometry was determined in similar titrations but using high receptor concentrations (2  $\mu\text{M}$ ). When the concentration of receptor exceeds the dissociation constant by a factor of 10 or more, extrapolations of limiting slopes of fluorescence values at low occupation and at saturation by ligand yield suitable estimates of stoichiometry.

For measurements of competition with other ligands, BCNI and receptor concentrations usually were 5.0 and 0.2  $\mu\text{M}$ , respectively. Data were plotted to the logarithmic formulation (3).

$$\log \left[ \frac{f_B - f}{f - f_C} \right] = n_H \log \frac{K_B}{K_C} + n_H \log \frac{[C]}{[B]} \quad (1)$$

where  $f$ ,  $f_B$ , and  $f_C$  are the observed BCNI fluorescence, the fluorescence when BCNI fully occupies all available sites on the receptor, and the fluorescence when BCNI is fully dissociated from the receptor (i.e., in the presence of excess competing ligand).  $[B]$  and  $[C]$  represent the BCNI and competing ligand concentrations, and  $K_B$  and  $K_C$  their respective dissociation constants. When  $[B]$  exceeds both the concentration of receptor sites and  $K_B$ ,  $[C]/[B]$  can be estimated from the concentrations of added ligand.

**Pharmacological properties of BCNI.** Procedures for measurement of ligand binding and activity as agonists and antagonists in the mammalian muscle cell line BC3H-1 have been previously described (24). The concentration dependence of BCNI in inhibiting the initial rate of  $\alpha$ -toxin binding yields a protection constant  $K_P$ .  $\alpha$ -Toxin binding to the receptors on the cell surface was measured at 20 sec following addition of  $\alpha$ -toxin. Labeled  $\alpha$ -toxin was added simultaneously with BCNI or after a 20-min exposure of the receptors to BCNI. The capacity of BCNI to inhibit carbamylcholine-elicited  $\text{Na}^+$  permeability was monitored by exposure of the cells to a specified concentration of BCNI for 20 min, followed by a test pulse of 60  $\mu\text{M}$  carbamylcholine, tracer  $^{22}\text{Na}^+$ , and the same concentration of BCNI. Initial rates of  $^{22}\text{Na}^+$  influx were measured at 15 sec after agonist addition. In the measurements of receptor occupation and functional antagonism, a  $\text{K}^+$ -Ringer's solution was employed (24) to minimize changes in membrane potential associated with agonist-elicited permeability changes.



**Assay of BCNI action by voltage clamp.** BCNI was tested for agonist and antagonist activities at AChRs by measurement of membrane conductance changes produced when the compound was iontophoretically applied to voltage-clamped reptilian neuromuscular junctions. These experiments were performed using twitch fiber end-plates from the costocutaneous muscles of garter snakes (sp. *Thamnophis*). The anatomy which suits these junctions for electrophysiological studies and the activation kinetics of these receptors have been described (25–27). The properties of these AChRs are virtually indistinguishable from those in *Torpedo* electric organ and BC3H-1 cells except that the snake receptors are insensitive to  $\alpha$ -toxin (26, 28). Intact costocutaneous muscles were removed from the animals and maintained in a physiological salt solution [composition (millimolar): NaCl 159, KCl 2.15,  $\text{CaCl}_2$  1.0,  $\text{MgCl}_2$  4.2, 4-(2-hydroxyethyl)-1-piperazineethanesulfonic acid 1.0; pH 7.2, 14–16°C]. End-plates were visualized with Nomarski optics and voltage-clamped with two low-resistance microelectrodes filled with 3 M KCl (26). BCNI was iontophoretically applied to the end-plate area from a pipette (nominally 10 Mohm) using a constant current controller; the pipette concentration of BCNI was about 0.5 M. Agonist actions were monitored as the ability of BCNI to increase membrane conductance through the activation of receptors. Antagonist actions were monitored by the effects which BCNI caused on spontaneously occurring miniature end-plate currents; miniature end-plate current frequency, amplitude, and time course were examined.

## RESULTS

**PMR spectra of BCNI.** Figure 1A shows the PMR spectrum of BCNI dissolved in deuterated water. Aside from the HOD peak at 4.7 ppm, the only impurity is acetonitrile at 1.96 ppm. Assignment of the 2.9 ppm triplet as a methylene  $\beta$  to the imino nitrogen was consistent through the whole series of ester compounds synthesized. A decoupling experiment (Fig. 1B) illustrates that the unresolved triplet at 4.19 ppm is coupled to the 2.9 ppm triplet and therefore must represent methylene groups  $\alpha$  to the imino nitrogen. The other two peaks at 3.67 ppm and 4.51 ppm are methylene groups at  $\alpha$  and  $\beta$ , respectively, on the choline portion of the ester. Finally, the quaternary methyl groups integrate for 18 protons and are appropriately located at 3.13 ppm.

**Inhibition of acetylcholinesterase.** Since acetylcholinesterase inhibitors are known to inhibit both the enzyme-catalyzed acylation and deacylation steps of ester (acetylcholine) hydrolysis to different extents, it has proven more convenient to select a substrate where inhibition of only the acylation step is examined. If carbamyl esters are used at moderate substrate concentrations, the relative rate of enzyme decarbamylation is sufficiently slow that it can be neglected in the analysis. Carbamylation of acetylcholinesterase by the nonfluorescent substrate *N*-methyl-7-dimethyl-carbamoyloxy-quinolinium releases an equivalence of the fluorescent 7-hydroxyquinolinium (21) and hence can be easily monitored (Fig. 2A). Although the reaction shows deviations from Michaelis-Menton kinetics at high substrate concentrations (cf. ref. 3), reciprocal plots over a limited substrate concentration range do reveal competitive inhibition for BCNI (Fig. 2B). Rather similar inhibitory behavior has been noted for the active site-selective ligand, edrophonium (3). An apparent  $K_i$  of  $4.6 \times 10^{-7}$  M for BCNI can be calculated from the relationship  $K_i = K_P/(1 + S/K_s)$ , where  $S$  and  $K_s$  are the substrate concentration and the dissociation constant for carbamylation.

We have also monitored BCNI hydrolysis over periods of several hours by sequential sampling and electropho-

retic separation of the individual products (Fig. 3A). In water, BCNI undergoes slow hydrolysis to the monoquaternary ester at a rate of less than 1% per hour (Fig. 3B). In the pH 8.0 buffer, the rate is enhanced to 14%/hr, whereas conversion to the diacid occurs more slowly (0.8%/hr). Addition of 2  $\mu\text{M}$  acetylcholinesterase to BCNI enhances the rate of conversion to the monoquaternary 3-fold (46%/hr), whereas hydrolysis of the monoquaternary ester is enhanced 6-fold to 5%/hour. In a separate experiment, hydrolysis of 140  $\mu\text{M}$  BCNI in buffer was found not to be enhanced by the addition of 1.8  $\mu\text{M}$  acetylcholinesterase which had been inhibited by diisopropyl fluorophosphate. Hence, the slow rate of enzyme-catalyzed hydrolysis of BCNI occurs at the active center and cannot be explained by general base catalysis at other residues on the enzyme surface.

**Fluorescent properties of BCNI.** Figure 4A shows the corrected excitation and emission spectra of BCNI in acetone and aqueous buffer. The quantum yield of BCNI in pH 7.4, 10 mM sodium phosphate buffer was 0.06 using fluorescein in 0.1 N NaOH ( $Q = 0.85$ ) as a standard and comparing areas of corrected emission curves. Hypsochromatic shifts of  $\sim 15$  nanometers of the excitation and emission spectra and 2-fold increases in quantum yield have been reported when primary amines of NBD are present in solvents of lower dipole moments (29). We found similar behavior for a secondary amine analogue of NBD.

When excess AChR is added to BCNI, a hypsochromatic shift occurs similar to that in acetone (14 nm), and an apparent  $\sim 25\%$  enhancement of fluorescence quantum yield (estimated from the areas under the emission spectra) is observed with excitation at 474 nm. Prior block of the sites with 1 mM carbamylcholine reveals a spectrum that is similar to BCNI in buffer (Fig. 4B). Hence, the enhancement and wavelength shift of BCNI fluorescence appear to be a consequence of association with carbamylcholine-protectable sites rather than binding to nonspecific sites or partitioning into the membrane component of the preparation.

Addition of acetylcholinesterase to BCNI reveals a decrease in its fluorescence at 527 nm when excited either at 290 nm or 474 nm. However, determination of BCNI fluorescence in the presence of excess enzyme can be expected to be complicated by partial hydrolysis of BCNI. To circumvent this problem, we have irreversibly inhibited acetylcholinesterase to greater than 99.8% by reaction with methanesulfonyl *N*-methylpyridinium (30). Formation of the methanesulfonyl-conjugated enzyme has been shown not to affect dissociation constants of bisquaternary ligands containing terminal quaternary methyl groups (30). The BCNI spectrum in the presence of 1.0  $\mu\text{M}$  methanesulfonyl acetylcholinesterase is shown in Fig. 4C. Separate titrations of 1.0 and 2.0  $\mu\text{M}$  BCNI over a concentration range 0.1–5.0  $\mu\text{M}$  methanesulfonyl acetylcholinesterase yield a maximal quenching of 68% of BCNI fluorescence (data not shown). The data are best fit by one BCNI site per 80,000  $M$ , subunit, a value in good accord with the stoichiometry of binding of the bisquaternary benzoquinone ligands (30).

**Fluorescence titration of acetylcholinesterase.** Conditions where BCNI is in excess over the enzyme will minimize hydrolysis of the ligand, and the most con-

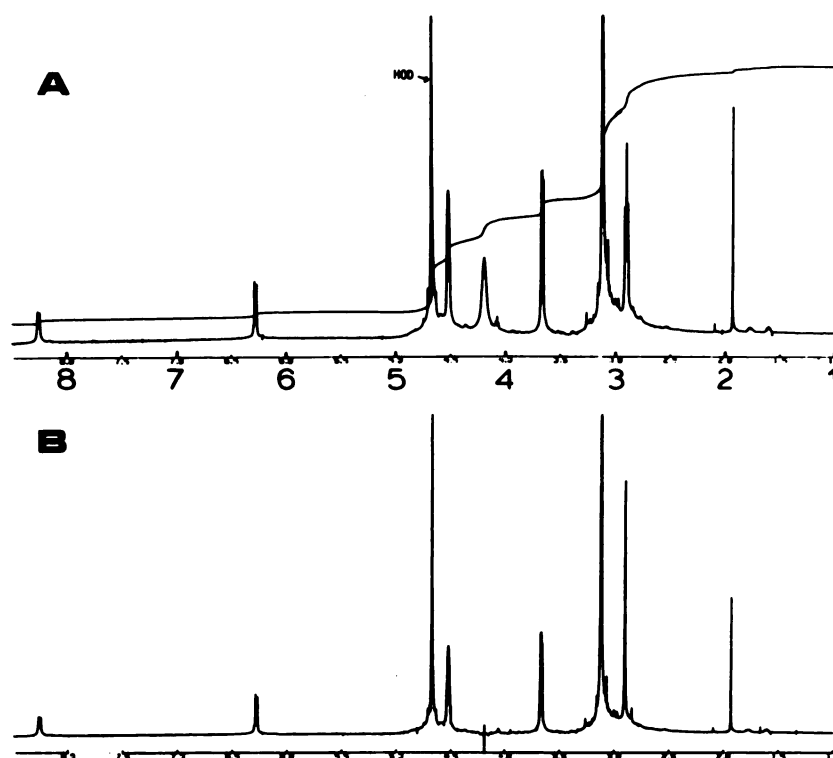
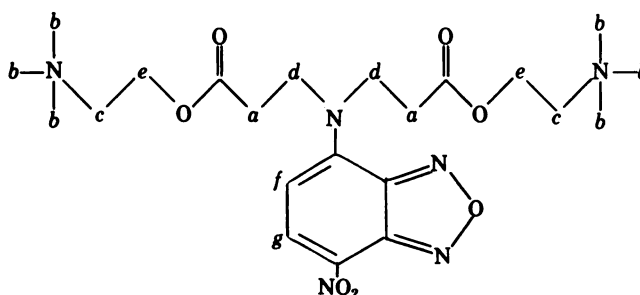


FIG. 1. Fourier-transform (FT) PMR spectra of BCNI at 500 MHz. BCNI concentration was 10 mg/ml dissolved in  $^2\text{H}_2\text{O}$ . A. Normal FT spectrum with integration. B. Decoupled spectrum. The methylene peak at 4.19 ppm was irradiated and splitting was eliminated at the methylene peak at 2.90 ppm.



a	2.90 ppm	4 protons	triplet $J = 7.5$ Hz
b	3.13 ppm	18 protons	singlet
c	3.67 ppm	4 protons	triplet $J = 5$ Hz
d	4.19 ppm	4 protons	unresolved triplet
e	4.51 ppm	4 protons	unresolved triplet
f	6.28 ppm	1 proton	doublet 10 Hz
g	8.26 ppm	1 proton	doublet 10 Hz

venient means of monitoring BCNI binding to unmodified acetylcholinesterase in the presence of excess ligand involves quenching of the enzyme tryptophanyl fluorescence. Owing to substantial overlap between the fluorescence emission of tryptophanyl residues on the enzyme and BCNI absorption at 340 nm, the quenching of protein (donor) fluorescence is a direct measure of BCNI (acceptor) association. A dissociation constant of  $0.2 \mu\text{M}$  is calculated from the titration curve, and the final BCNI-acetylcholinesterase fluorescence possesses 60% of the fluorescence of unbound acetylcholinesterase (Fig. 5).

**BCNI association with the AChR.** The capacity of BCNI to associate with the purified membrane fragments

containing AChR was initially ascertained from inhibition of the initial rates of  $\alpha$ -toxin binding. For spin-labeled analogues of decamethonium, these competition measurements yielded dissociation constants equivalent to those ascertained directly by spin resonance spectrometry (6). When the initial rate of  $\alpha$ -toxin binding is measured over 20-sec intervals immediately following addition of BCNI, the apparent  $K_P$  is  $0.26 \mu\text{M}$  (Fig. 6). When BCNI is added to the receptor 20 min prior to addition of  $\alpha$ -toxin, the protection constant,  $K_P$ , is  $0.11 \mu\text{M}$ , a reduction of slightly more than 2-fold. The enhanced competition between ligand and  $\alpha$ -toxin following exposure to ligand is a consequence of a slow transition to a receptor state with higher affinity for the ligand

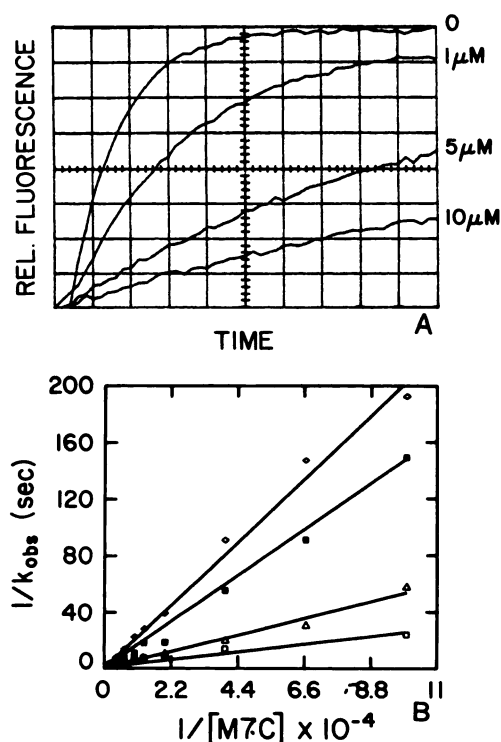


FIG. 2. BCNI Inhibition of acetylcholinesterase carbamylation by 7-(dimethylcarbamoyl)*N*-methylquinolinium (M7C)

Acetylcholinesterase (AChE) (0.2 μM) was mixed with the designated concentrations of BCNI in 10 mM Tris-HCl containing 0.1 N NaCl and 40 mM MgCl<sub>2</sub> (pH 8.0). M7C (100 μM) was then added, and fluorescence was monitored at 510 nm with excitation at 410 nm. A Durrum stopped-flow instrument was employed for admixture of reactants and detection. Amplified photomultiplier currents were fed into an A/D converter coupled with a Tektronix 4051 computer. Data were analyzed as a first-order approach to an equilibrium fluorescence value. A. Relative fluorescence enhancement due to M7C production monitored by stopped flow in the absence and presence of the indicated BCNI concentrations. Each large increment on the abscissa is 5 sec. At lower substrate concentrations ( $\leq 10$  μM), decarbamylation rates become significant relative to carbamylation and the equilibrium value was assigned by extrapolation. B. Reciprocal plots of the rate constant and substrate concentration: □, no BCNI; Δ, 0.5 μM BCNI; ■, 2.5 μM BCNI; ◇, 5 μM BCNI. Each point represents an average of duplicate determinations. The line represents a simple linear regression fit to the data. For the scheme



$k_2 = 0.224 \text{ sec}^{-1}$  and  $K_c = 49 \text{ μM}$ .

(6, 31–33). This conversion in state as reflected in an enhanced binding affinity has been observed previously for agonists and certain (metaphilic) antagonists (6, 32, 33).

**Fluorescence titration of the AChR.** Titration of the membrane-associated receptor with BCNI shows approximately a 2-fold enhancement of BCNI fluorescence at 519 nm when excited at 474 nm (cf. Fig. 4B). However, the enhancement of signal of the bound ligand is increased more than 40-fold with excitation at 290 nm. Although BCNI itself has a smaller fluorescence contribution when excited at 290 nm, the tryptophanyl residues in the protein are also excited at 290 nm, and their emission at 340 nm overlaps with an excitation band of

BCNI in this region (cf. Fig. 4). The spectral overlap favors dipolar fluorescence energy transfer from the receptor tryptophanyl residues to BCNI. This feature greatly augments detection of bound species.

Direct fluorescence titrations of AChR by BCNI (cf. Fig. 7A) indicate association of BCNI to a single class of AChR receptor sites. Separate fluorescence titrations at high receptor concentrations ( $>2.0$  μM) show a stoichiometry of  $0.90 \pm 0.16$  BCNI sites to one α-toxin site. Analysis of binding by Hill plots yields slopes in the range between 0.9 and 1.45 mean ( $1.16 \pm 0.14$ ) with a dissociation constant of  $0.23 \pm 0.03$  μM (Table 1). The

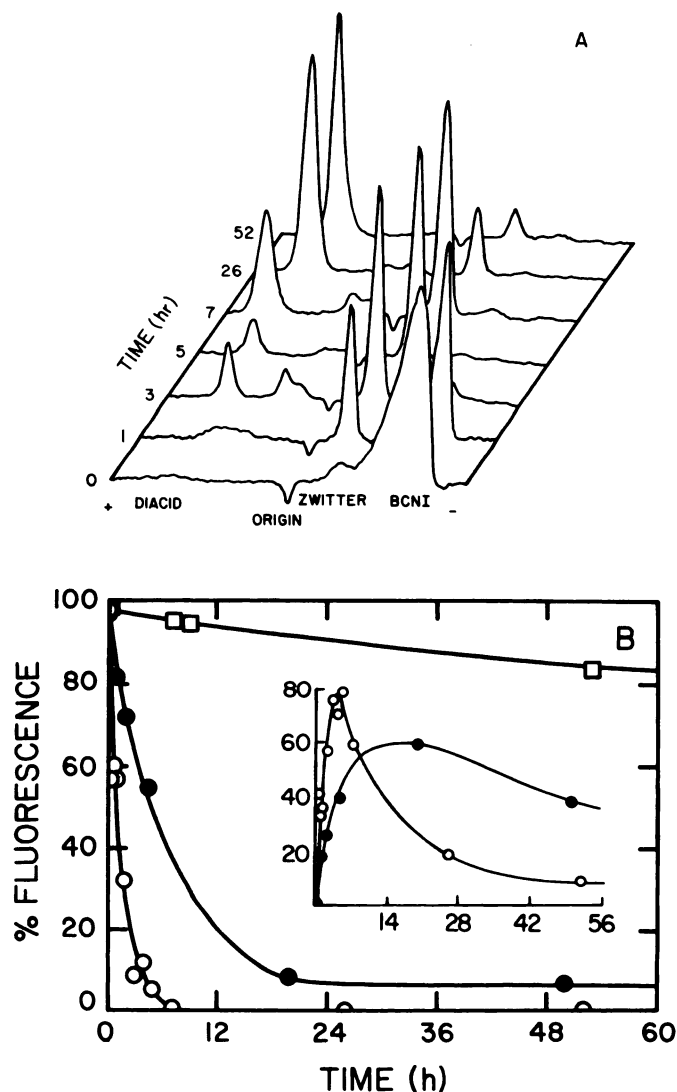


FIG. 3. Measurement of hydrolysis of BCNI by acetylcholinesterase. BCNI (140 μM) and acetylcholinesterase (2 μM) in 0.1 M NaCl, 40 mM MgCl<sub>2</sub>, and 10 mM Tris-HCl (pH 8.0) were mixed and incubated at 25° for the designated time. Samples were removed and subjected to electrophoresis on cellulose acetate as specified under Methods. A. The diester moves to the cathode, the zwitterionic monoester remains near the origin, and the completely hydrolyzed product (the diacid) moves toward the anode. The individual species were quantitated using a fluorescent scanner. B. Disappearance kinetics of BCNI: □, hydrolysis in water; ●, hydrolysis in the above buffer; ○, hydrolysis in the presence of 2 μM acetylcholinesterase. Inset, appearance and disappearance of the zwitterionic monoester (●), hydrolysis in buffer (○), and hydrolysis in the presence of 2 μM acetylcholinesterase.



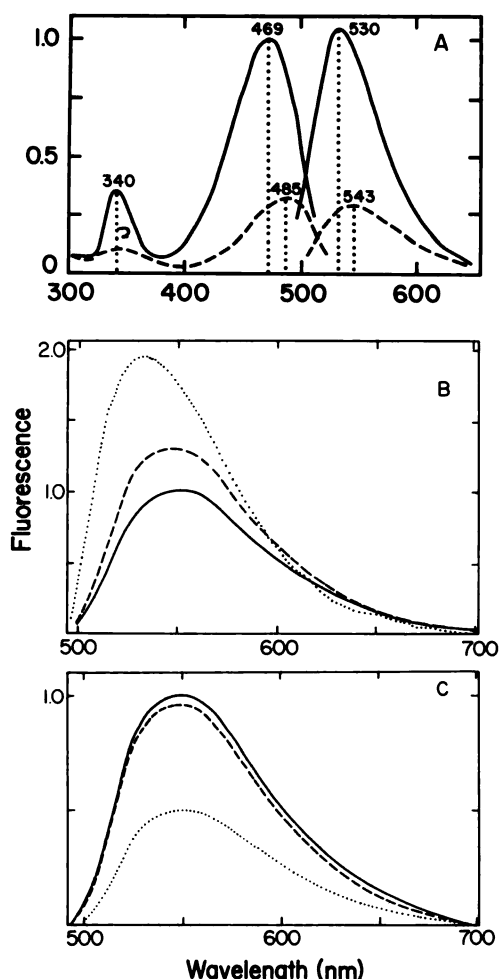


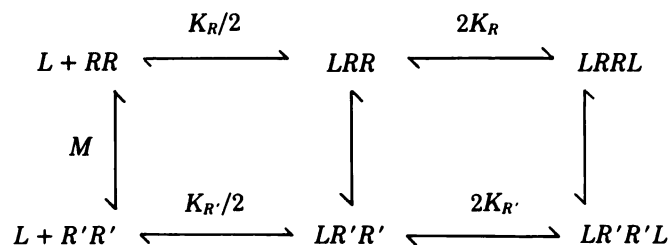
FIG. 4. Effect of solvent and association with acetylcholinesterase and the AChR on BCNI fluorescence

A. Corrected excitation and emission spectra of BCNI in 10 mM Tris-HCl buffer (pH 8.0) containing 0.1 M NaCl and 40 mM MgCl<sub>2</sub> (---) and in acetone (—). Emission and excitation spectra were recorded with the emission and excitation monochromators set at peak wavelengths. The calculated molar extinction coefficient of BCNI at 485 nm is  $2.9 \times 10^4$  in the above buffer. B. Corrected emission spectra of 1.0 μM BCNI in the above buffer alone ( $\lambda_{\text{max}}$  547 nm) (—), with the membrane-associated AChR 2.0 μM in α-toxin sites ( $\lambda_{\text{max}}$  533 nm) (.....), with the same receptor preparation containing 1 mM carbamylcholine ( $\lambda_{\text{max}}$  547 nm) (---), excitation at 474 nm. Light scatter contributions to the spectra were corrected from a separate measurement of the spectrum of the receptor preparation in the absence of BCNI. The fluorescence intensities of BCNI with receptor in the presence and absence of carbamylcholine were compared directly; however, only the spectral profiles and not the absolute intensities can be compared for BCNI measured in the presence and absence of receptor owing to reductions of incident and emitted light. The reduction in intensity due to light scatter has been estimated from titrations of 1 μM BCNI with excess receptor (1–4 μM). C. Corrected emission spectra of BCNI (1.0 μM) in buffer (—), in 1.0 μM methanesulfonyl acetylcholinesterase (.....) and 1 μM methanesulfonyl acetylcholinesterase containing 1.0 mM decamethonium (---). Assuming a dissociation constant of 0.2 μM, approximately 65% of the BCNI is bound. Light scatter is insignificant in the case of acetylcholinesterase.

latter constant is in close accord with values estimated from competition with the initial rate of α-toxin binding (Fig. 6).

Since considerable evidence exists for two interconvertible receptor states with different affinities for ago-

nists, binding data were also fit to the reaction scheme below in which two states of a receptor containing two binding sites predominate.



SCHEME 1

$K_R$  and  $K_{R'}$  represent dissociation constants for the  $R$  and  $R'$  states;  $M = R'/R$  and is the allosteric constant which specifies the population of the two receptor states in absence of ligand. Although with *Torpedo* receptor, cooperativity of the binding of agonists has been found to be small (6) and hence simpler schemes can fit the binding data, in the mammalian receptor, cooperativity in agonist binding is more evident and a two-site concerted scheme is necessary to accommodate the data (4, 34, 35). Since there are two primary binding sites for α-toxin or agonist per receptor molecule (cf. 3, 35, 36), the above scheme can be universally employed to model the slower binding steps.

In Scheme 1 the state function for ligand binding,  $\bar{Y}$ , is described as follows:

$$\bar{Y} = \frac{\frac{A}{K_R} \left(1 + \frac{A}{K_R}\right) + M \frac{A}{K_{R'}} \left(1 + \frac{A}{K_{R'}}\right)}{\left(1 + \frac{A}{K_R}\right)^2 + M \left(1 + \frac{A}{K_{R'}}\right)^2} \quad (2)$$

The Hill coefficients we have obtained in titrations of several membrane preparations exhibit a mean value of 1.16; this indicates minimal apparent cooperativity in binding. To obtain  $K_R$  and  $K_{R'}$  we utilized a general nonlinear least-squares regression program based on the Gauss Newton method with Hartley's modification (37). The two-state:two-site model described by Eq. 2, fit to the data in Fig. 7B, was statistically compared with the fit for the simpler single-site, two-state model. When the allosteric constant  $M$  was set to 0.1, a value determined independently for our buffer conditions in previous studies (6), the minimization routine converged on estimates of  $K_R = 0.23 \pm 0.03$  μM and  $K_{R'} = 0.051 \pm 0.004$  μM for the data in Fig. 7. A general linear test comparing the residual sum of squares for fits to the two models gave  $\alpha(1) = 0.0025$  from an  $F$  statistic of 12.5 for a numerator of 1 and a denominator of 25 (38). Although the statistically improved fit cannot be taken as evidence that Scheme 1 provides the best description of the fluorescence titration data, it does allow us to assign dissociation constants to a model which is supported by prior kinetic findings (cf. refs. 3, 5, 35, and 36). The ratio of  $K_R/K_{R'}$  of 4.5 for BCNI is far smaller than the ratios of  $K_R/K_{R'}$  recorded for full agonists in the same system and is comparable with that found for partial agonists or certain antagonists (32). In the experiments with BCNI inhibi-

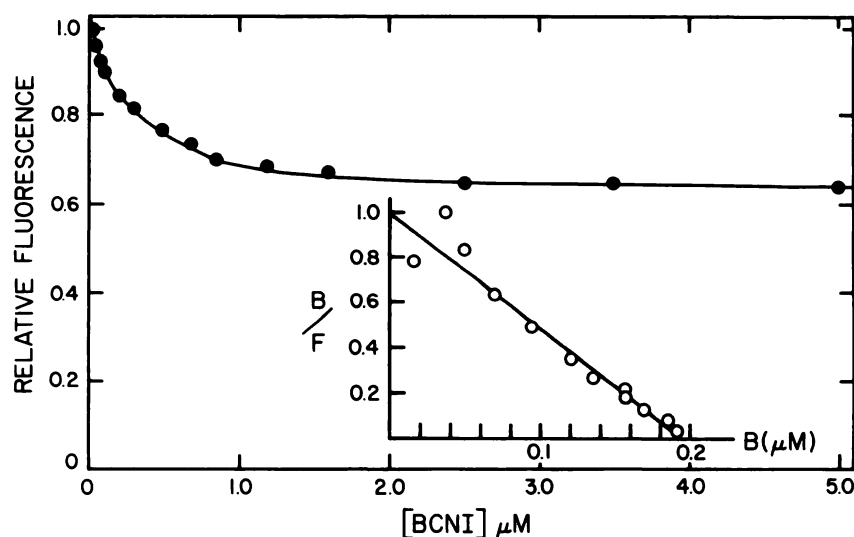


FIG. 5. BCNI quenching of acetylcholinesterase fluorescence

Incremental quantities of BCNI were added to a solution of  $0.2 \mu\text{M}$  acetylcholinesterase (active sites) in  $10 \text{ mM}$  Tris-HCl containing  $0.1 \text{ N}$  NaCl and  $40 \text{ mM}$   $\text{MgCl}_2$  (pH 8.0). Fluorescence of the enzyme tryptophanyl residues is monitored at  $340 \text{ nm}$  with excitation at  $290 \text{ nm}$  and corrections made for dilution and inner filter effects. Inset, Scatchard plot of the same data. Maximal fluorescence quenching was ascertained from reciprocal plots of the data.  $K_d = 1.9 \times 10^{-7} \text{ M}$ .

tion of  $\alpha$ -toxin binding,  $K_{p,\text{inst}}$  (the protection constant measured immediately after BCNI addition) should approach  $K_R$  whereas  $K_{p,\text{equil}}$  (measured following a 20-min exposure to BCNI) should be bounded by  $K_R$  and  $K_{R'}$ . The ratio of  $K_{p,\text{inst}}/K_{p,\text{equil}}$  of 2.4 as well as their absolute values are in good accord with the values calculated in the titration experiments.

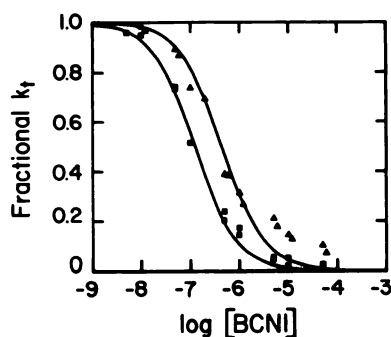


FIG. 6. Competition of BCNI for the initial rate of cobra  $\alpha$ -toxin binding to the membrane-associated AChR

Details on the assay procedure are given under Methods, and the rate constants for  $\alpha$ -toxin association are estimated from the fractions bound at several times over the initial 40-sec interval. ▲, Receptor-containing membranes ( $45 \text{ nM}$  in  $\alpha$ -toxin sites; specific activity =  $2 \text{ nM}$   $\alpha$ -toxin sites per milligram of protein) in  $10 \text{ mM}$   $\text{NaPO}_4$  (pH 7.4) and  $100 \text{ mM}$  NaCl were exposed to the specified concentrations of BCNI for 10 sec prior to initiation of the  $\alpha$ -toxin reaction, ■, the same membranes were exposed to BCNI for 20 min prior to initiation of the  $\alpha$ -toxin binding reaction. The observed rates are plotted versus the BCNI concentration and fit to the equation

$$Y = 1 - \frac{[L]}{[L] + K_i}$$

For no prior exposure  $K_i = 2.6 \times 10^{-7} \text{ M}$ , and for 30-min prior exposure  $K_i = 1.1 \times 10^{-7} \text{ M}$ . Some deviation from the above equation is seen for BCNI at high concentrations and after short exposure.

To ascertain whether the binding and concomitant fluorescence enhancement of BCNI are consequences of its binding solely to the agonist/antagonist site, we have monitored dissociation of BCNI by various agonists and antagonists (Fig. 8) and then determined whether analysis of competitive dissociation will yield dissociation constants for the competing ligands in accord with those measured by inhibitors of the  $\alpha$ -toxin binding rate. As shown in Table 1 and Fig. 8A and C, agonists, partial agonists, and antagonists dissociate BCNI from its binding site. In the presence of excess competing ligands, the resultant BCNI fluorescence upon  $290 \text{ nm}$  excitation is equivalent to the summation of the fluorescence of unbound BCNI and the light scatter contribution of the receptor (Fig. 8A). The very low concentrations of receptor ( $0.2 \mu\text{M}$ ) required with excitation at  $290 \text{ nm}$  minimize the errors incurred from light scatter. Dissociation constants for the various agonists determined from the fluorescence competition experiments show good agreement with those estimated previously from competition with the initial rates of  $\alpha$ -toxin binding (Table 1). Back titration with alkaloid antagonists yielded less reliable data. The absorption of *d*-tubocurarine at  $290 \text{ nm}$  created a substantial inner filter effect which obscured signal differences in the high concentration range. Pancuronium back titrations yielded a Hill coefficient less than unity which reflected the inequivalence of its presumed two binding sites on the receptor molecule (32, 39). Hill coefficients less than unity were previously observed with pancuronium inhibition of the initial rate of  $\alpha$ -toxin binding (32); however, we have not observed close correlations in binding constants using the two methods. The precision of the titrations is compromised by the low concentrations of receptor required to titrate the high-affinity site and the large concentration range of pancuronium employed.

Binding of BCNI appears selective for the agonist-



antagonist site, since the local anesthetic, lidocaine, does not cause appreciable dissociation of BCNI at concentrations up to  $10^{-3}$  M and, in fact, at lower concentrations causes a slight enhancement of fluorescence (Fig. 8B). Previous studies have shown that local anesthetics enhance the binding affinity of agonists for the membrane-associated receptor (6). Many local anesthetics appear to

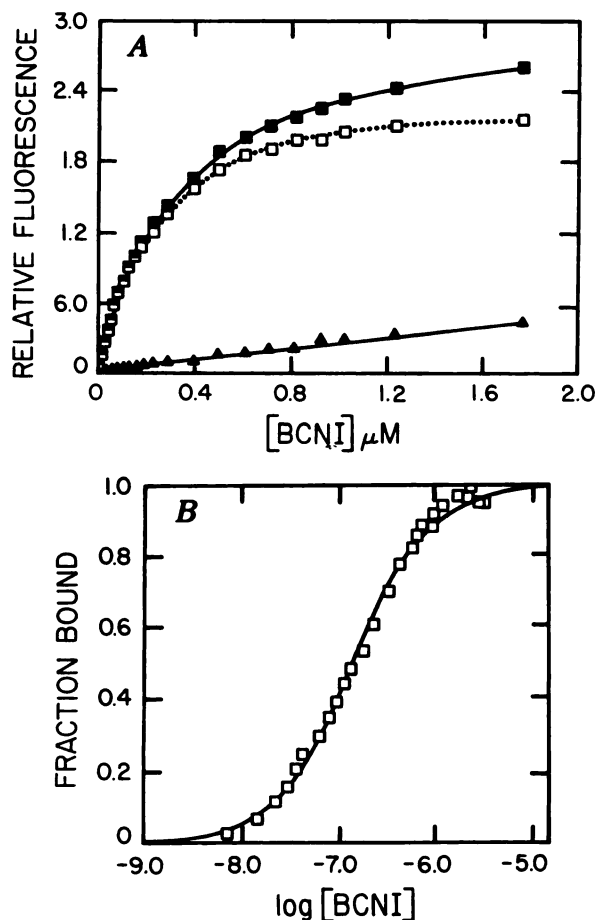


FIG. 7. Titration of BCNI with the membrane-associated AChR

To 2 ml of a membrane suspension of the AChR ( $0.1 \mu$ M in  $\alpha$ -toxin sites) in 10 mM  $\text{NaPO}_4$  (pH 7.4) and 100 mM NaCl were added incremental quantities of BCNI. A. Fluorescence was measured at 519 nm with excitation at 290 nm.  $\blacksquare$ — $\blacksquare$ , membranes without prior treatment;  $\blacktriangle$ — $\blacktriangle$ , membranes exposed to 1 mM carbamylcholine prior to and during the titration;  $\square$  . . . .  $\square$ , the two curves subtracted to yield specific binding. B. Plot of titration data as percentage of receptor bound plotted against the concentration of free ligand. The line represents the best fit to Eq. 3. A nonlinear least-squares analysis is employed, where  $M$  is fixed at 0.1 and  $K_R$  and  $K_R'$  are optimized to achieve a minimization of residuals. In this case  $K_R = 0.230 \pm 0.31 \mu$ M and  $K_R' = 0.051 \pm 0.004 \mu$ M. The residual sum of squares for this model was compared using a general linear test (38) to a two-state model for single-site binding. An  $F$  statistic = 12.5 was calculated from the following equation and results in 99.75% confidence in the full model:

$$\frac{SS_p - SS_f}{SS_f} \times \frac{(N - p)}{k} = F[k, N - p, \alpha(1)]$$

where  $SS_p$  = residual sum of squares for the partial model,  $SS_f$  = residual sum of squares for the full model,  $N$  = number of data points,  $p$  = number of parameters in the partial model, and  $k$  = number of parameters in the full model  $- p$ .

TABLE 1

Fluorescence titrations of BCNI with the membrane-associated receptor

Direct titration				
Preparation	$K_D^a$	$n_H^a$		
Receptor	$0.22 \pm 0.03 \mu\text{M}$	$1.16 \pm 0.14$ (5)		
Receptor + $4 \times 10^{-4}$ M lidocaine	$0.15 \pm 0.03 \mu\text{M}$	$1.11 \pm 0.09$ (5)		
Competitive titrations with BCNI				
Competing ligand	Fluorescence competition <sup>a,b</sup>		Protection against $\alpha$ -toxin binding <sup>c</sup>	
	$K_C$	$n_H$	$K_p$	$n_H$
Carbamylcholine	$0.28 \pm 0.03 \mu\text{M}$ (4)	$1.09 \pm 0.09$	$0.48 \mu\text{M}$	1.11
Decamethonium	$1.41 \pm 0.3 \mu\text{M}$ (3)	$0.98 \pm 0.12$	$0.83 \mu\text{M}$	1.0
Suberyldicholine	$0.0036 \pm 0.0006 \mu\text{M}$ (3)	$1.11 \pm 0.07$	$0.004 \mu\text{M}$	—
Pancuronium	$0.18 \pm 0.04 \mu\text{M}$ (4)	$0.48 \pm 0.08$	$0.04 \mu\text{M}$	0.32

<sup>a</sup> Mean  $\pm$  standard error (number of titrations is given in parentheses).

<sup>b</sup> Calculated according to Eq. 1; titrations were conducted with  $5.0 \mu$ M BCNI and 0.1 or  $0.2 \mu$ M receptor.

<sup>c</sup>  $K_p$ , the protection constant, and the associated Hill coefficient,  $n_H$ , were determined from the inhibition of the initial rate of  $\alpha$ -toxin binding (cf. ref. 6).

act as heterotropic, allosteric ligands and increase the allosteric constant  $M$  (4, 35, 36). Hence by increasing the ratio of  $R'/R$ , a greater fraction of the receptor is in a state possessing a higher affinity for agonists. For lidocaine under these conditions, the half-maximal concentration affecting this conversion in state is  $2 \times 10^{-5}$  M (6). In paired titrations we observe small enhancements of BCNI affinity in the presence of  $10^{-4}$  M lidocaine, but we have not detected a significant change in the Hill coefficient for BCNI binding when conducted in the presence and absence of lidocaine (Table 1).

**Pharmacological properties of BCNI.** To ascertain whether BCNI behaves as an agonist or antagonist, we have examined its behavior in two systems responsive to nicotinic agonists. In BC3H-1 cells, BCNI does not elicit a detectable increase in  $\text{Na}^+$  permeability between  $10^{-7}$  and  $10^{-5}$  M. In the same system, suberyldicholine exhibits maximal increases in permeability comparable to acetylcholine and carbamylcholine, whereas permeability elicited by the partial agonist, decamethonium, is 11% of that of suberyldicholine (34). In our assay it is possible to detect permeability responses that are 1% of those of suberyldicholine. BCNI binding to the receptor in BC3H-1 cells can be demonstrated from competition with  $\alpha$ -toxin binding or antagonism of carbamylcholine-elicited  $\text{Na}^+$  permeability (Fig. 9), and it appears to be less potent as an antagonist with the mammalian receptor than in the *Torpedo* receptor.

In the snake neuromuscular junction we examined BCNI for both agonist and antagonist activities by monitoring the junctional membrane conductance during iontophoretic application. BCNI caused no detectable change in membrane conductance under conditions where a full agonist such as acetylcholine should have produced at least a  $10^{-6}$  S change in conductance; our resolution was better than  $5 \times 10^{-9}$  S. Furthermore, using fluctuation analysis we found no increase in current noise. However, BCNI reversibly blocked spontaneous miniature end-plate currents in a dose-dependent manner in this preparation (Fig. 10). Blockade was manifest as a reduced amplitude, whereas the decay time constant of miniature end-plate currents was unchanged by BCNI

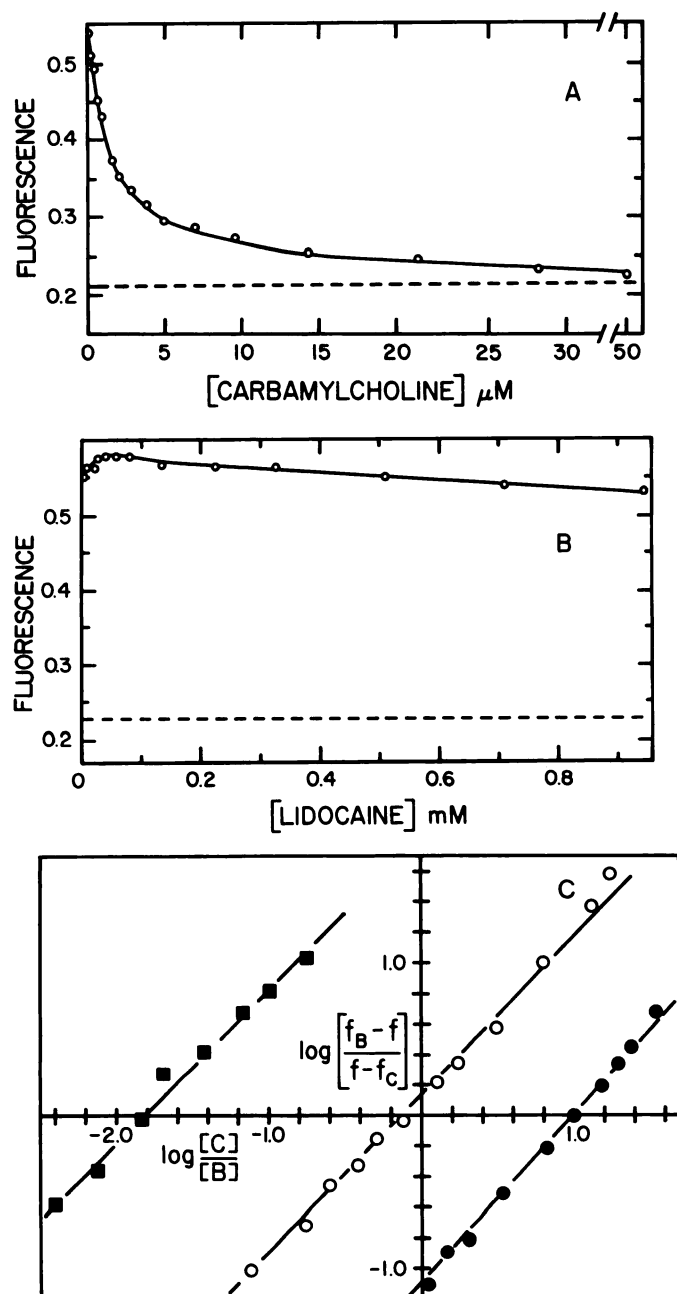


FIG. 8. Back titration of the BCNI-AChR complex by agonists and local anesthetics

Conditions are the same as in Fig. 7. A. BCNI (1.5 μM) was added to the receptor-containing membranes (0.5 μM in α-toxin sites), and incremental quantities of carbamylcholine were added. B. BCNI (1.5 μM) was added to the receptor-containing membranes (0.5 μM in α-toxin sites), and incremental quantities of lidocaine were added. C. Plot of back titrations of BCNI fluorescence with decamethonium (●—●), carbamylcholine (○—○), and suberyldicholine (■—■), according to Eq. 1.  $f$ ,  $f_B$ , and  $f_c$  represent the observed fluorescence, fluorescence with BCNI alone, and  $f_c$  fluorescence in the presence of excess competing ligand.  $[B]$  and  $[C]$  are the concentrations of BCNI and competing ligand, respectively. To ensure that the free BCNI concentration was nearly constant during the titration, either 0.1 or 0.2 μM receptor and 5.0 μM BCNI were employed in most of the titrations of Table 1 and those shown in C.

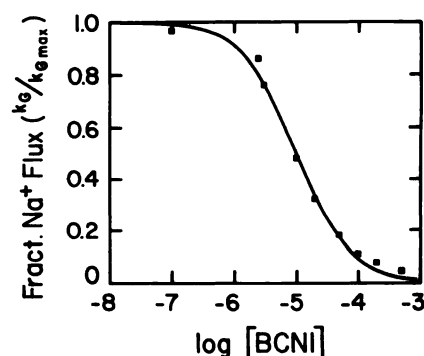


FIG. 9. Antagonism of carbamylcholine-elicited <sup>22</sup>Na<sup>+</sup> permeability by BCNI

BC3H-1 muscle cells were grown to confluence (14 days after passage) and washed twice over a 30-min interval in K<sup>+</sup>-Ringer's buffer. The buffer was then aspirated and BCNI at the designated concentration was added to the culture dishes. After 20 min the BCNI-containing buffer was aspirated, and a buffer containing BCNI at the same concentration, 60 μM carbamylcholine, and tracer <sup>22</sup>Na<sup>+</sup> was added for 10 sec. The reaction was abruptly stopped with two 3-ml washes of 0.5 mM d-tubocurarine in K<sup>+</sup>-Ringer's buffer followed by two 3-ml washes of K<sup>+</sup>-Ringer's buffer. Cells were then immediately removed from the plates with a 3% Triton X-100 solution and counted. Data are plotted relative to the Na<sup>+</sup> influx in the absence of BCNI. The curve is fitted to the equation  $Y = 1 - ([BCNI]/[BCNI + IC_{50}])$ , where  $IC_{50} = 10$  μM.

concentrations that were sufficient to produce nearly total suppression of peak current. Such behavior is characteristic of competitive antagonists.

## DISCUSSION

**Synthesis.** The synthetic procedure for BCNI was developed after unsatisfactory yields with several shorter synthetic schemes. The NBD moiety appears to be labile under basic conditions. Hydrolysis of the dinitrile in HCl did not go to completion. Thus, the methyl ester was formed by using methanol and H<sub>2</sub>SO<sub>4</sub>. Formation of the diacid could be driven to completion in 2-butanone by removal of methanol as an azeotrope with water. Transesterification of the methyl ester to form the bromoethyl ester was unsuccessful. Carbodiimides, thionyl chloride, and oxalylchloride proved inferior to trifluoroacetic acid anhydride in activating the diacid. Scrupulously dry conditions must be employed in the final step, and the handling of BCNI is made difficult by its hygroscopic nature.

**BCNI association with acetylcholinesterase.** Bisquaternary ligands in which approximately 14 Å or 10 methylene groups separate the quaternary nitrogens bind with one-to-one stoichiometry to each subunit on acetylcholinesterase (30). Also, substantial evidence has accrued that one quaternary nitrogen binds to an anionic subsite of the active center whereas the interquaternary chain and the second quaternary nitrogen are directed away from the active site serine (esteratic subsite) on each subunit. The enzyme can be irreversibly inactivated by methanesulfonyl fluoride when bisquaternary ligands are bound (40). Moreover, alkanesulfonation and dialkylphosphorylation of the enzyme affect binding of these bisquaternary inhibitors only when the alkyl groups are

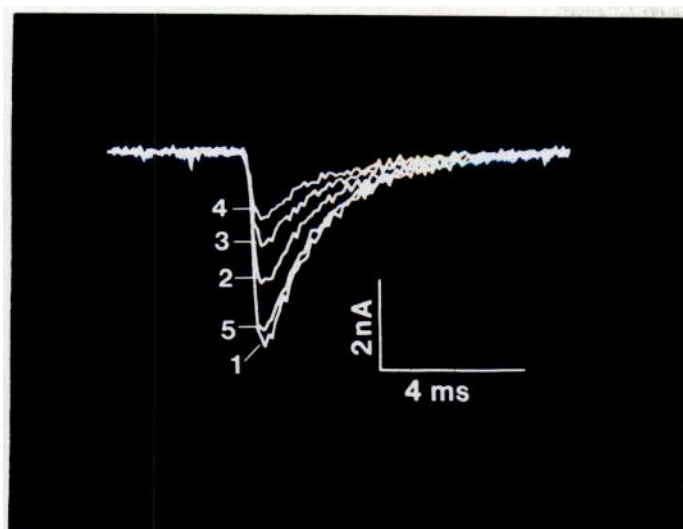
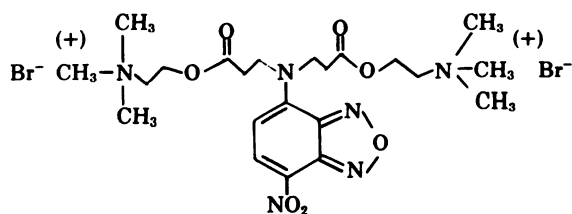


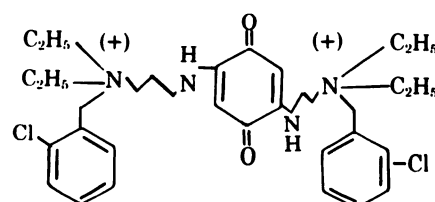
FIG. 10. BCNI antagonism of spontaneous miniature end-plate currents

BCNI reversibly reduced the amplitude of miniature end-plate currents at the snake neuromuscular junction but did not alter their time course. Each trace is the mean of 11–20 miniature end-plate currents, all from the same cell recorded in the presence of different concentrations of BCNI. The sequence of measurements began with the largest (most negative peak) current (trace 1), recorded with no BCNI as a control. Iontophoretic backing current was then reduced in steps to three levels which produced partial reduction in the end-plate current amplitude (traces 2, 3, and 4); as more BCNI was released from the pipette, a greater depression of the mean negative peak current was observed. Finally, we returned the iontophoretic current to its control value to record the recovered response (trace 5). Between each new setting of the iontophoretic current we waited 30 sec before recording new data. Temperature: 14.4°. The decay time constants of these five mean responses were as follows: 1, 0.57; 2, 0.55; 3, 0.54; 4, 0.50; 5, 0.55 reciprocal msec.

sufficiently large to encroach on the anionic subsite (30). Finally, equivalent fluorescent quenching with incremental occupation of each of the sites suggests that the bisquaternary ligands do not span between the subunits (30). The 1:1 stoichiometry, the slow rate of BCNI hydrolysis, and the extent of fluorescence quenching suggest that BCNI subsumes an orientation similar to that of other bisquaternary ligands when associated with acetylcholinesterase. To illustrate this point, it is instructive to compare the fluorescence quenching obtained with BCNI and the 2,5-bis[trialkylammonio-*n* propylamino]-benzoquinones studied previously (30). Both chromophores are equidistant between the quaternary groups.



bis-(Choline)N-[4 nitrobenzo-2-oxa-1,3-diazol-7-yl]imino dipropionate



2,5-bis[3-Diethyl-(3-o-chlorobenzyl)ammonio-*n*-propylamino]benzoquinone

Measurement of enzyme fluorescence quenching by BCNI and the benzoquinone ligands can be used to calculate their respective weighted average distances from the array of tryptophanyl residues on the enzyme. If both chromophores occupy similar positions on the enzyme surface, this calculation should yield equivalent donor-to-acceptor distances when normalized to their respective spectroscopic overlap integrals. In the case of the benzoquinone moiety, 53% quenching is observed with a calculated overlap integral of  $16.9 \times 10^{-15} \text{ cm}^6/\text{mole}$ , whereas with BCNI 40% quenching is observed with a calculated overlap integral of  $7.9 \times 10^{-15} \text{ cm}^6/\text{mole}$ .  $R_0$ , the critical transfer distance at 50% quenching efficiency, may be calculated from the equation below:

$$R_0(\text{\AA}) = 9.79 \times 10^3 (J \kappa^2 n^{-4} Q)^{1/6} \quad (3)$$

where  $J$  is the overlap integral ( $\text{cm}^6/\text{mole}$ ),  $\kappa^2$  is the orientation factor (0.67),  $n$  is the refractive index (1.6), and  $Q$  is the donor quantum yield (0.121). Substitution of the respective overlap integrals into Eq. 3 yields values of 23.9 Å for the bisquaternary benzoquinone and 21 Å for BCNI.

Very good agreement is then found for the weighted average distances,  $R$ , of the benzoquinone ligands and BCNI from the matrix of tryptophanyl residues as calculated from the fractional quenching,  $E$  and  $R_0$ , according to the following equation (41):

$$R = (1/E - 1)^{1/6} R_0$$

For BCNI,  $R = 22.5 \text{ \AA}$ , and for the bisquaternary benzoquinone,  $R = 23.4 \text{ \AA}$ .

It should be recognized that  $R$  as a weighted average distance between the ligand chromophore and several tryptophanyl residues cannot be realistically interpreted in structural terms. Nevertheless, if the NBD chromophore of BCNI and the benzoquinone chromophore of benzoquinonium assume overlapping positions on the macromolecule surface, we should expect close agreement in the calculated values of  $R$ .

In previous studies, hydrolysis of mono-NBD acylcholine was examined by fluorescence methods (42). These ligands were also found to exhibit a reduction in fluorescence when bound to acetylcholinesterase. The monoquaternary ester NBD 5-acylcholine, while a far poorer substrate than acetylcholine ( $k_{\text{cat}} = 0.07$  versus 8000 moles/sec/mole of acetylcholinesterase) appears to be a better substrate than the BCNI diester ( $k_{\text{cat}} = 0.009$  moles/sec/mole of acetylcholinesterase). Steric constraints in the acyl pocket of the active center of the enzyme render all of the acylcholines as poor substrates.



That the bisquaternary choline esters are even poorer substrates could well be due to the orientation of the bound ligand away from the active site serine in the active center.

**BCNI association with the AChR.** Although we were disappointed that our strategem of retaining carbonyl groups between the two quaternary groups as in suberyldicholine did not lead to formation of a compound which was an agonist, BCNI possesses properties desirable for future studies on the receptor. First, its high affinity and one-to-one stoichiometry with  $\alpha$ -toxin sites indicate that BCNI enjoys specificity for a single type of binding site. This is confirmed by the observations that only agonists and antagonists will dissociate BCNI from the receptor and competition with local anesthetics is not observed. While measurements were made on different receptor preparations, the electrophysiological measurements and the inhibition of agonist-elicited  $\text{Na}^+$  permeability in BC3H-1 cells also point to BCNI's being a competitive antagonist. Second, the enhanced fluorescence of BCNI in the bound state renders this compound useful in fluorescence polarization or energy transfer studies. Third, the location of the fluorophore in the BCNI molecule ensures that the position of the chromophore with respect to the subsites binding the quaternary groups is fixed. In contrast, *N*-substitution of a fluorophore at one of the quaternary groups in bisquaternary ligands would lead to an asymmetrical molecule with two distinct binding orientations. With its fixed binding position and minimal conformational flexibility when bound, BCNI should prove useful in estimating intersite distances on the receptor molecule (22).

The dissociation constants for BCNI binding to the agonist-antagonist site show good agreement between measurements of ligand competition with the initial rate of  $\alpha$ -toxin binding and the equilibrium fluorescence titrations. The difference in protection constants against the rate of  $\alpha$ -toxin binding observed for BCNI with immediate and prolonged BCNI exposure to the receptor differ by a factor of 2.4 in the *Torpedo* receptor. This compares with values of 30 for most agonists and values that approach unity for certain antagonists (32). Similarly, the ratio of dissociation constants,  $K_R/K_{R'}$ , determined according to Eq. 2, differ by a factor of 4.5 whereas this ratio is approximately 300 for full agonists. The ratio of dissociation constants found for BCNI resembles that of other bisquaternary compounds, among which the metaphilic antagonists would be included (32, 33). Thus, in such an analysis BCNI exhibits a slight preference for binding to the desensitized state of the receptor. The 1:1 stoichiometry observed would indicate that the conversion in state effected by BCNI is mediated simply by binding to the agonist-antagonist sites on the receptor and not by simultaneous association with the agonist-antagonist site and an allosteric site.

A recent study demonstrated that NBD-5 acylcholine binds to two sites in equal abundance on the AChR from *Electrophorus* with dissociation constants that differ by a factor of 100 (43). However, it is difficult to make direct comparisons between the two studies, since the aforementioned investigation was conducted on a detergent-solubilized receptor. Solubilization is known to have a

marked effect on the dissociation constants of bound ligands (4, 35, 36).

**Spectroscopic behavior of bound BCNI.** Upon excitation at 474 nm, an apparent ~25% enhancement of fluorescence quantum yield and a 14 nm hypsochromatic shift of the NBD spectrum is seen when BCNI is bound to the AChR (Fig. 4). With excitation at 290 nm, where energy transfer occurs between the protein tryptophanyl residues serving as donors and the acceptor, BCNI, 40-fold increases in fluorescence are observed (Fig. 8). In contrast, the NBD moiety of BCNI when bound to acetylcholinesterase exhibits a diminution of fluorescence and the absence of a substantial shift in wavelength when compared with the free fluorophore. The lack of fluorescence enhancement would suggest that the NBD moiety associated with acetylcholinesterase is not bound within a hydrophobic pocket but rather is either in a hydrophilic environment or in a charge-transfer complex with an aromatic residue on the enzyme surface. In contrast, the NBD moiety is likely to be associated with a hydrophobic surface on the receptor which gives rise to the substantial fluorescence enhancement and shift to lower wavelength. Both the AChR and acetylcholinesterase show remarkably similar specificities for bisquaternary ligands (44). For both macromolecules the inhibitory properties of these ligands become maximal when the interquaternary distance approaches 14 Å (17, 18, 45). Yet, despite these similarities in binding specificities and affinities, our spectroscopic studies show that the respective binding surfaces of the two macromolecules involved in bisquaternary ligand complex formation differ strikingly.

## REFERENCES

- Weber, G., D. Borris, E. DeRobertis, F. Barrantes, J. LaTorre, and M. DeCarlin. The use of a cholinergic receptor probe for the study of receptor proteolipid. *Mol. Pharmacol.* 7:530-536 (1971).
- Mooser, G., and D. S. Sigman. Ligand binding properties of acetylcholinesterase determined with fluorescent probes. *Biochemistry* 13:2299-2307 (1974).
- Taylor, P., and S. Lappi. Interaction of fluorescence probes with acetylcholinesterase: the site and specificity of propidium binding. *Biochemistry* 14:1989-1997 (1975).
- Changeux, J. P. The acetylcholine receptor: an allosteric membrane protein. *Harvey Lect.* 75:85-254 (1981).
- Weber, M., and J. P. Changeux. Binding of *Naja nigricollis* [ $^3\text{H}$ ] $\alpha$ -toxin to membrane fragments from *Electrophorus* and *Torpedo* electric organs. *Mol. Pharmacol.* 10:35-40 (1974).
- Weiland, G., B. Georgia, S. Lappi, C. F. Chignell, and P. Taylor. Kinetics of agonist-mediated transitions in state of the cholinergic receptor. *J. Biol. Chem.* 252:7648-7656 (1977).
- Epstein, D. J., H. A. Berman, and P. Taylor. Ligand-induced conformational changes in acetylcholinesterase investigated with fluorescent phosphonates. *Biochemistry* 18:4749-4754 (1979).
- Bolger, M. B., and P. Taylor. Kinetics of association between bisquaternary ammonium ligands and acetylcholinesterase: evidence for two conformational states of the enzyme from stopped-flow measurements of fluorescence. *Biochemistry* 18:3622-3629 (1979).
- Grunhagen, H. H., M. Iwatsubo, and J.-P. Changeux. Fast kinetic studies on the interaction of cholinergic agonists with the membrane-bound acetylcholine receptors from *Torpedo marmorata* as revealed by quinacrine fluorescence. *Eur. J. Biochem.* 80:225-242, (1977).
- Heidmann, T., and J. P. Changeux. Fast kinetic studies on the interaction of a fluorescent agonist with the membrane bound acetylcholine receptor from *Torpedo marmorata*. *Eur. J. Biochem.* 94:255-279 (1979).
- Jüress, R., H. Prinz, and A. Maelicke. NBD-5 Acylcholine: fluorescent analog of acetylcholine, an agonist at the neuromuscular junction. *Proc. Natl. Acad. Sci. U. S. A.* 76:1064-1068 (1979).
- Grunhagen, H. H., and J.-P. Changeux. Studies on the electrogenic action of acetylcholine with *Torpedo marmorata* electric organ IV. *J. Mol. Biol.* 106:497-516 (1976).

13. Cohen, J. B., and J.-P. Changeux. Interaction of a fluorescent ligand with membrane bound cholinergic receptor of *Torpedo marmorata*. *Biochemistry* 12:4855-4864 (1973).
14. Barrantes, F. J., B. Sakmann, R. Bonner, H. Eibl, and T. M. Jovin. 1-Pyrenebutylcholine: a fluorescent probe for the cholinergic system. *Proc. Natl. Acad. Sci. U. S. A.* 72:3097-3101 (1975).
15. Waksman, G., J.-P. Changeux, and B. P. Rogues. Agonist and blocking properties of new acylcholine analogues. *Mol. Pharmacol.* 18:20-27 (1980).
16. Adams, P. R., and B. Sakmann. Decamethonium both opens and blocks endplate channels. *Proc. Natl. Acad. Sci. U. S. A.* 78:2994-2998 (1978).
17. Barlow, R. B., and H. R. Ing. Curare-like action of polymethylene bisquaternary ammonium salts. *Br. J. Pharmacol.* 3:298-304 (1949).
18. Barlow, R. B., and A. Zoller. Activity of analogues of decamethonium on the chick biventer cervicis preparation. *Br. J. Pharmacol.* 19:485-491 (1962).
19. Adams, P. R. Relaxation experiments using bath-applied suberyldicholine. *J. Physiol. (Lond.)* 268:271-290 (1979).
20. Taylor, P., J. W. Jones, and N. M. Jacobs. Acetylcholinesterase from *Torpedo*: characterization of enzyme species isolated by lytic procedures. *Mol. Pharmacol.* 10:78-92 (1974).
21. Rosenberry, T. L., and S. Bernhard. Studies of catalysis by acetylcholinesterase: synergistic effects of inhibitions during hydrolysis of acetic acid esters. *Biochemistry* 11:4308-4321 (1972).
22. Johnson, D. A., J. G. Voet, and P. Taylor. Fluorescence energy transfer between cobra  $\alpha$ -toxin molecules bound to the acetylcholine receptor. *J. Biol. Chem.* 259:5717-5725 (1984).
23. Berman, H. A., J. Yguerabide, and P. Taylor. Fluorescence energy transfer on acetylcholinesterase spatial relationship between peripheral site and active center. *Biochemistry* 19:2226-2235 (1980).
24. Sine, S., and P. Taylor. Functional consequences of agonist-mediated state transitions in the cholinergic receptor. *J. Biol. Chem.* 254:3315-3325 (1979).
25. Kulchitsky, N. Nerve endings in muscles. *J. Anat. (Lond.)* 58:152-169.
26. Dionne, V., and R. L. Parsons. Characteristics of acetylcholine-operated channel at twitch and slow fibre neuromuscular junctions of the garter snake. *J. Physiol. (Lond.)* 310:145-158 (1981).
27. Dionne, V. The kinetics of slow muscle acetylcholine operated channels in the garter snake. *J. Physiol. (Lond.)* 310:159-190 (1981).
28. Burden, S. J., H. C. Hartzell, and D. Yoshikami. Acetylcholine receptors at neuromuscular synapses: phylogenetic differences detected by snake  $\alpha$ -neurotoxins. *Proc. Natl. Acad. Sci. U. S. A.* 72:3245-3249 (1975).
29. Lancet, D., and I. Pecht. Spectroscopic and immunochemical studies with nitrobenzoxadiazolealanine, a fluorescent dinitrophenyl analogue. *Biochemistry* 16:5150-5157 (1977).
30. Taylor, P., and N. M. Jacobs. Interaction between bisquaternary ammonium ligands and acetylcholinesterase—complex formation studied by fluorescence quenching. *Mol. Pharmacol.* 10:93-107 (1974).
31. Weber, M., T. David-Pfeuty, and J.-P. Changeux. Regulation of binding properties of the nicotinic receptor protein by cholinergic ligands in membrane fragments from *Torpedo marmorata*. *Proc. Natl. Acad. Sci. (U. S. A.)* 72:3443-3447 (1975).
32. Weiland, G., and P. Taylor. Ligand specificity of state transitions in the cholinergic receptor: behavior of agonists and antagonists. *Mol. Pharmacol.* 15:197-212 (1979).
33. Rang, H. P., and J. M. Ritter. A new kind of drug antagonism: evidence that agonists cause a molecular change in acetylcholine receptors. *Mol. Pharmacol.* 5:394-411 (1969).
34. Sine, S. M., and P. Taylor. The relationship between agonist occupation and the permeability response of the cholinergic receptor revealed by bound cobra  $\alpha$ -toxin. *J. Biol. Chem.* 255:10144-10156 (1980).
35. Karlin, A. Molecular properties of nicotinic acetylcholine receptors, in *The Cell Surface and Neuronal Function* (G. Pate, G. L. Nicolson, and C. W. Cotman, eds.) Elsevier, Amsterdam, 191-260 (1980).
36. Taylor, P., R. D. Brown, and D. A. Johnson. The linkage between occupation and response of the nicotinic acetylcholine receptor. in *Topics in Membranes and Transport* (A. Kleinzeller and B. R. Martin, eds.) Vol. 15. Academic Press New York, 407-443 (1983).
37. Hartley, H. O. The modified Gauss Newton method for the fitting of nonlinear regression functions by least squares. *Technometrics* 3:269 (1961).
38. Boxenbaum, H. G., S. Riegelman, and R. M. Elashoff. Statistical estimation in pharmacokinetics. *J. Pharmacokinet. Biopharm.* 2:123 (1974).
39. Neubig, R. R., and J. B. Cohen. Equilibrium binding of [ $^3$ H]d-tubocurarine and [ $^3$ H]acetylcholine by *Torpedo* post-synaptic membranes: stoichiometry and ligand interactions. *Biochemistry* 18:5456-5475 (1979).
40. Belleau, B., V. DiTullio, and Y.-H. Tsai. Kinetic effects of leptocurares and pachycurares on the methane sulfonylation of acetylcholinesterase. *Mol. Pharmacol.* 6:41-45 (1970).
41. Förster, T. In *Modern Quantum Chemistry* (O. Sinanoglu, ed.), Part 3. Academic Press, New York, 93-99 (1956).
42. Jürrs, R., and A. Maelicke. Interaction of acetylcholinesterase with fluorescence analogues of acetylcholine. *J. Biol. Chem.* 256:2887-2893 (1981).
43. Prinz, H., and A. Maelicke. Interaction of cholinergic ligands with the purified acetylcholine receptor protein. *J. Biol. Chem.* 258:10263-10271 (1983).
44. Paton, W. D. M., and E. J. Zaimis. The pharmacological actions of polymethylene bistrimethylammonium compounds. *Br. J. Pharmacol. Chemother.* 4:381-400 (1949).
45. Changeux, J.-P. Responses of acetylcholinesterase from *Torpedo marmorata* to salts and curarizing drugs. *Mol. Pharmacol.* 2:369-392 (1966).

Send reprint requests to: Dr. Palmer Taylor, Division of Pharmacology, M-013H, Department of Medicine, University of California, San Diego, La Jolla, Calif. 92093.